united nations educational, scientific and cultural organization

international atomic energy agency

the
abdus salam
international centre for theoretical physics

Winter College on Optics and Photonics
7 - 25 February 2000

1218-25

"2nd Order Nonlinear Optics"

F. LAURELL
Royal Institute of Technology
Stockholm, Sweden

2nd order nonlinear optics

Fredrik Laurell
Royal Institute of Technology
Stockholm, Sweden

2. NONLINEAR OPTICS

2.1. Introduction.

This chapter will give a basic theoretical description of the principal second-order nonlinear interactions that give rise to energy transfer between different frequencies. The presentation in sections 2.2. and 2.3.1-3 is similar to Yariv's treatment [43]. In this context a comparison between the expressions for the conversion efficiency for plane waves and gaussian beams is made. Possibilities to obtain efficient interaction by using birefringence phase-matching and quasi-phase-matching are discussed.

2.2. Formalism for nonlinear interaction with planar waves

It is possible to deduce a compact description of energy transfer between different frequencies from Maxwell's equations,

$$\nabla \times \mathbf{H} = \mathbf{J} + \frac{\partial}{\partial t}(\varepsilon_0 \mathbf{E} + \mathbf{P}), \tag{2.1.a.}$$

$$\nabla \times \mathbf{E} = -\frac{\partial}{\partial t}(\mu \mathbf{H}), \tag{2.1.b}$$

where $\mathbf{E}$ and $\mathbf{H}$ are the instantaneous electric and magnetic vectors, $\mathbf{J}$ is the electric current density , μ is the permeability tensor and the polarization vector $\mathbf{P}$ is given by a linear and a nonlinear term as:

$$\mathbf{P} = \varepsilon_0 \chi_L \mathbf{E} + \mathbf{P}_{NL}, \tag{2.2}$$

$$(P_{NL})_i = 2\varepsilon_0 d_{ijk} E_j E_k. \tag{2.3}$$

These equations can be combined to the nonlinear wave equation:

$$\nabla^2 \mathbf{E} = \mu_0 \sigma \frac{\partial \mathbf{E}}{\partial t} + \mu \varepsilon_0 \varepsilon_r \frac{\partial^2 \mathbf{E}}{\partial t^2} + \mu \frac{\partial^2}{\partial t^2} \mathbf{P}_{NL}. \tag{2.4}$$

To simplify the solution of the wave equation, assume that the electric field consists of plane waves at three frequencies, ω_1, ω_2 and ω_3, propagating in the z direction only,

$$E_1(z,t) = \frac{1}{2}\left[E_1(z) e^{i(\omega_1 t - k_1 z)} + c.c.\right]$$

$$E_2(z,t) = \frac{1}{2}\left[E_2(z) e^{i(\omega_2 t - k_2 z)} + c.c.\right] \tag{2.5}$$

$$E_3(z,t) = \frac{1}{2}\left[E_3(z) e^{i(\omega_3 t - k_3 z)} + c.c.\right].$$

One can easily solve (2.4) by using the slowly varying field approximation and assuming a transparent medium ($\sigma = 0$). In the special case where the frequencies have been chosen $\omega_1 = \omega_3 - \omega_2$, the solution will be:

Solution for plane waves in lossless medium

$$\begin{aligned}\frac{dE_{1i}}{dz} &= -i\omega_1\sqrt{\frac{\mu\varepsilon_0}{\varepsilon_1}}d_{ijk}E_{3j}E_{2k}^{*}e^{-i(k_3-k_2-k_1)z}\\ \frac{dE_{2k}^{*}}{dz} &= +i\omega_2\sqrt{\frac{\mu\varepsilon_0}{\varepsilon_2}}d_{kij}E_{1i}E_{3j}^{*}e^{-i(k_1-k_3+k_2)z}\\ \frac{dE_{3j}}{dz} &= -i\omega_3\sqrt{\frac{\mu\varepsilon_0}{\varepsilon_3}}d_{jik}E_{1i}E_{2k}e^{-i(k_1+k_2-k_3)z}\end{aligned} \tag{2.6}$$

This is the general form of the solution to the nonlinear wave equation for plane waves in a lossless material.

2.3. Second-harmonic generation

The form of three-wave interaction that is simplest to treat is second-harmonic generation (SHG) in which two of the frequencies, ω_1 and ω_2, are equal. Here they are referred to as the fundamental angular frequency ω_F, while $\omega_{SH} = 2\omega_F$, is called the second-harmonic angular frequency. To change the description in (2.6) to fit this case, *i.e.* a fundamental field E_F and a second-harmonic field, E_{SH}, the nonlinear coefficient has to be divided by two in the last equation in (2.6), to compensate for the degeneracy when the power in the fundamental wave is divided on both E_1 and E_2. Furthermore, for a weak nonlinear process without depletion of the fundamental wave $\left(\frac{dE_F}{dz} = 0\right)$, the last equation in (2.6) can be written:

$$\frac{dE_{SH}}{dz} = -i\omega_F\sqrt{\frac{\mu\varepsilon_0}{\varepsilon_{SH}}}d_{eff}E_FE_Fe^{i\Delta kz}. \tag{2.7}$$

Here

$$\Delta k = k_{SH} - 2k_F, \tag{2.8}$$

represents the "phase mismatch" between the fundamental and second-harmonic waves. Note that d_{jik} has been exchanged for the relevant nonlinear coefficient, d_{eff}.

Integration of E_{SH} in (2.7) over the interaction length L, assuming no seeded second-harmonic ($E_{SH}(0) = 0$), gives the second-harmonic field as:

$$E_{SH}(L) = -i\omega_F\sqrt{\frac{\mu\varepsilon_0}{\varepsilon_{SH}}}d_{eff}E_F^2\frac{e^{i\Delta kz}-1}{i\Delta k}. \tag{2.9}$$

The intensity of the second-harmonic wave is given by Poynting's vector:

$$I_{SH} = \frac{P_{SH}}{A} = \frac{1}{2}\sqrt{\frac{\varepsilon_0\varepsilon_{SH}}{\mu}}E_{SH}E_{SH}^{*}, \tag{2.10}$$

where I_{SH} and P_{SH} stand for the second-harmonic intensity and power, respectively, and A is the effective transverse area over which the interaction takes place.

Inserting (2.9) in (2.10) one gets the second-harmonic intensity:

$$I_{SH}(L) = \frac{P_{SH}}{A} = 8\frac{\mu^{3/2}\sqrt{\varepsilon_0}\,\omega_F^2}{\varepsilon_F\sqrt{\varepsilon_{SH}}}d_{eff}^2L^2\frac{P_F^2}{A^2}\frac{\sin^2\frac{1}{2}\Delta kL}{\left(\frac{1}{2}\Delta kL\right)^2}. \tag{2.11}$$

Introducing the two basic relations:

$$c = \frac{1}{\sqrt{\mu_0 \varepsilon_0}}, \qquad n = \sqrt{\varepsilon_r \mu_r}, \tag{2.12}$$

one obtains the final expression for the conversion efficiency,

$$\eta = \frac{P_{SH}}{P_F} = 2\frac{\omega_F^2}{n_F^2 n_{SH} c^3 \varepsilon_0} d_{eff}^2 L^2 I_F \frac{\sin^2\left(\frac{1}{2}\Delta k L\right)}{\left(\frac{1}{2}\Delta k L\right)^2}, \tag{2.13}$$

or in terms of power,

$$\eta = \frac{P_{SH}}{P_F} = 2\frac{\omega_F^2}{n_F^2 n_{SH} c^3 \varepsilon_0} d_{eff}^2 L^2 \frac{P_F}{A} \frac{\sin^2\left(\frac{1}{2}\Delta k L\right)}{\left(\frac{1}{2}\Delta k L\right)^2}. \tag{2.14}$$

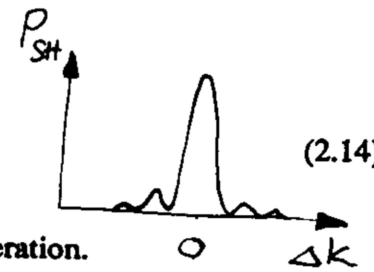

These are the general equations for second-harmonic generation.

2.3.1. Phase-matching in second-harmonic generation

The phase-matching condition should, in general, be fulfilled for an efficient energy transfer between the fundamental and the second-harmonic wave, *i.e.*;

$$\Delta k = k_{SH} - 2k_F = 0. \tag{2.15}$$

If $\Delta k = 0$, the sinc-term in the expression for the generated second-harmonic power will be equal to one, but in all other cases the efficiency will be lower. When the two waves propagate together through the crystal with the same phase velocity phase-matching is achieved, which means that they experience equal refractive indices.

If the phase-matching condition is not fulfilled, then the two waves propagate with different phase-velocities, so that, at some distance ($z = L$), the polarization, locally induced at the second-harmonic frequency by the fundamental signal, will be out of phase with the arriving second-harmonic radiation generated just at the input face of the crystal ($z = 0$). When the induced polarization is 180° out of phase with the propagating second-harmonic wave, the energy will couple back to the fundamental wave and the second-harmonic power will decrease. Hence, only a short length will be effective in the generation of second-harmonic radiation.

The crystal length that is useful in producing second-harmonic radiation is called the coherence length, l_c and is deduced from the argument of the sinc-function,

$$l_c = L \text{ in } \Delta k L = 2\pi,$$

which gives (2.16)

$$l_c = \frac{2\pi}{\Delta k}.$$

2.3.4. Periodic structures for phase-matching

Already in the early days of nonlinear optics it was suggested that periodic structures could be used to overcome the restrictions of the phase-matching condition [45],[112]. The technique is known as quasi-phase-matching (QPM). A spatial modulation is here used to compensate for the phase velocity mismatch between the interacting waves. In second-harmonic generation this means that the wave-vector mismatch,

$$\Delta k = 2k_{\omega} - k_{2\omega} \tag{2.23}$$

between the fundamental and the second-harmonic waves is compensated by the "momentum" of the spatial modulation,

$$\Delta k = m\frac{2\pi}{\Lambda}, \tag{2.24}$$

where Λ represents the periodicity of the spatial modulation and m is an integer giving the order of the periodicity. Both the linear properties, *i.e.* the refractive index, and the nonlinear properties can be modulated to obtain the required compensation of the momentum. Taking both theoretical aspects and realistic implementations under consideration, one finds that only modulation of the nonlinear properties will be effective [B]. In that case the expression for the conversion efficiency (2.14) will be different:

$$\eta = \frac{P_{SH}}{P_F} = 2\frac{\omega_F^2}{n_F^2 n_{SH} c^3 \varepsilon_0} L^2 \frac{P_F}{A} d_{QPM}^2, \tag{2.25}$$

where the active nonlinear coefficient, d_{QPM}, depends on how the nonlinearity is modulated. In the most efficient form of modulation, the sign of the nonlinear coefficient is changed every half coherence length,

$$\frac{l_c}{2} = \frac{\pi}{\Delta k}. \tag{2.26}$$

In second-harmonic generation this corresponds to a change of the coupling coefficient each time the two waves come completely out of phase (180°), and the second-harmonic power can continue to grow instead of being coupled back to the fundamental wave. The effective nonlinear coefficient will be equal to the relevant nonlinear coefficient multiplied by the Fourier component of the spatial modulation. For 50/50 laminar structures the expression will be,

$$d_{QPM} = \begin{cases} \dfrac{2}{m\pi} d_{eff} & \text{for odd m} \\ 0 & \text{for even m} \end{cases} \tag{2.27}$$

By inserting (2.27) in (2.25) one arrives at the plane-wave solution for quasi-phase-matching in laminar structures with complete modulation of the nonlinear coefficient,

$$\eta = \frac{P_{SH}}{P_F} = 8\frac{\omega_F^2}{m^2\pi^2 n_F^2 n_{SH} c^3 \varepsilon_0} L^2 \frac{P_F}{A} d_{eff}^2 \tag{2.28}$$

The highest efficiency is achieved when the spatial modulation is of first order ($m = 1$). It will be drastically reduced when higher-order modulation is used, which also can be seen in Fig. 2.1.

Advantage with periodically poled media

* phasematch all wavelength within transparency
* noncritical phasematching - no walk-off
* access d_{33} coefficient - > 10x
* Type I phasematching
* reduced photorefractive effect

PERIODICALLY POLED CRYSTALS FOR BULK QUASI-PHASEMATCHING

Applications

* in IR generation - OPOs and DFG
* SHG to visible and UV

~~Previously~~ studied crystals

$LiNbO_3$

+ reproducible process
- high poling fields (>20kV/mm) thin crystals 0.5 mm
- difficult to generate dense gratings

$LiTaO_3$

similar to $LiNbO_3$

shorter wavelengths with chemically patterned crystals

KTP ($KTiOPO_4$)

+ low poling voltage (2kV/mm)thick crystals >1mm
((only hydrothermally grown crystals work well))

RTA ($RbTiOAsO_4$)

+ flux grown crystals can be poled
- availability
- inhomogenities
- crystal size

RTP , CTA

GENERAL PROPERTIES OF KTP ISOMORPHS

* high nonlinearity
* high damage threshold
* low susceptibility to photorefractive damage

FOR POLING

* one dimensional structure
* low poling voltage

ROYAL INSTITUTE OF TECHNOLOGY

INSTITUTE OF OPTICAL RESEARCH

Temperature and Wavelength Tuning

Green generation

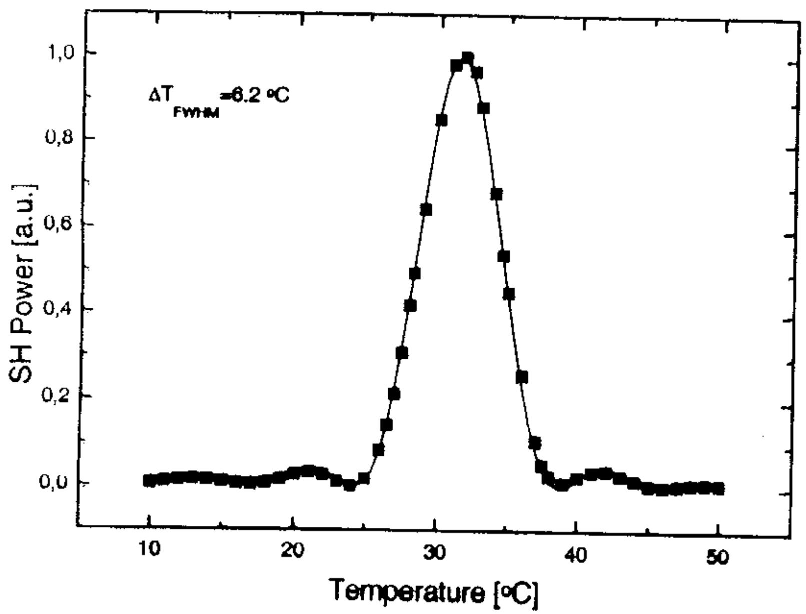

UV generation

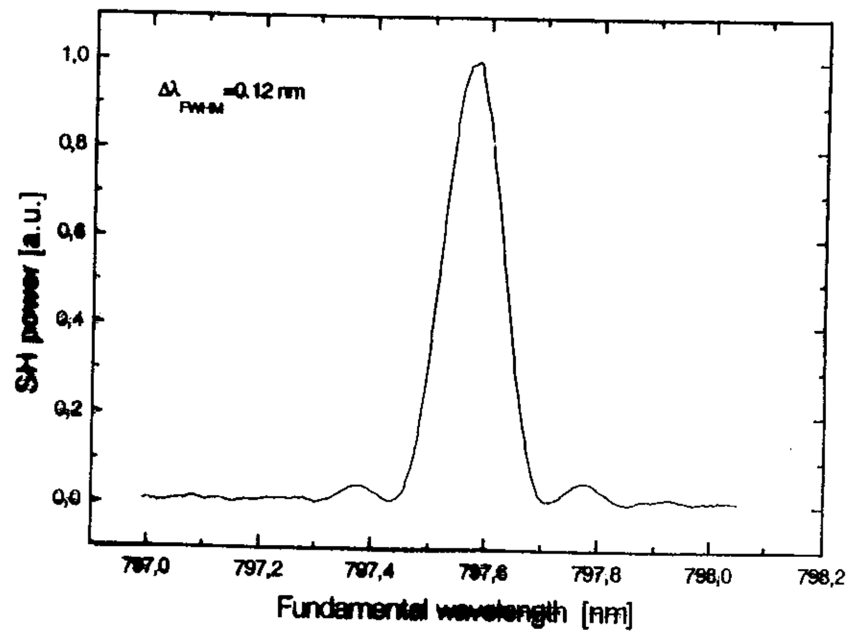

VETENSKAP OCH KONST

7.7 mm PPKTP

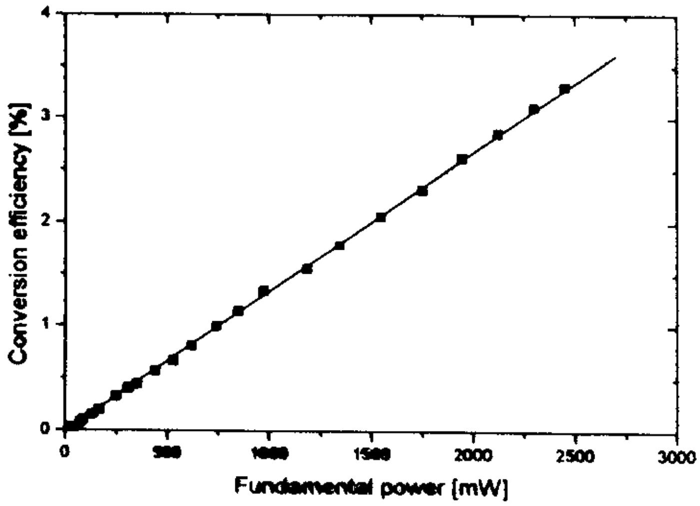

CW Nd:YAG
1.7%$W^{-1}cm^{-1}$

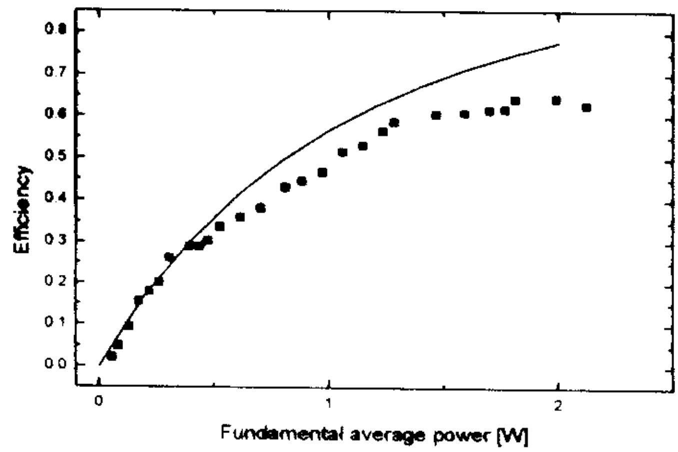

Mode-locked Nd:YAG
τ_p=100 ps
f_{rep}=100 MHz
w_0=22 μm
η=64%

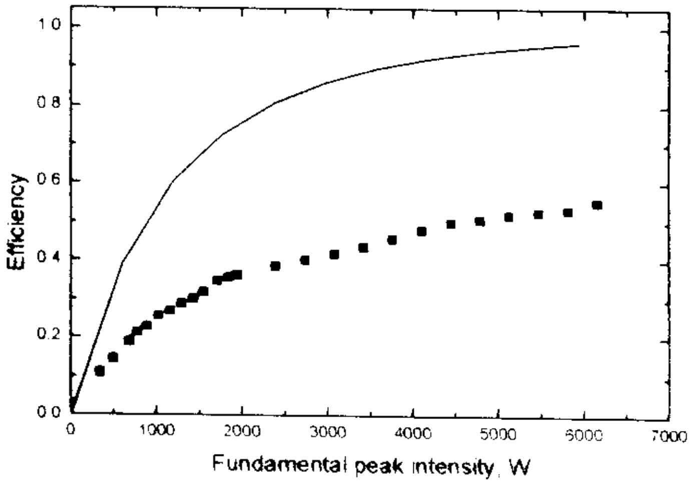

Q-switched Nd:YAG
τ_p=220 ns
f_{rep}=1 kHz
w_0=67 μm
η=56%

$$\eta \equiv \frac{P_{SH}}{P_F} = \tanh^2\left[(\gamma P_F)^{1/2}\right]$$

Frequency Doubling the Q-Switched Nd:YAG Lasers

$\tau_{pulse} = 5\ ns,$ *Single Pulse*

$W_{SH}^{max} = 2\ mJ, \quad \eta^{max} = 74\%$

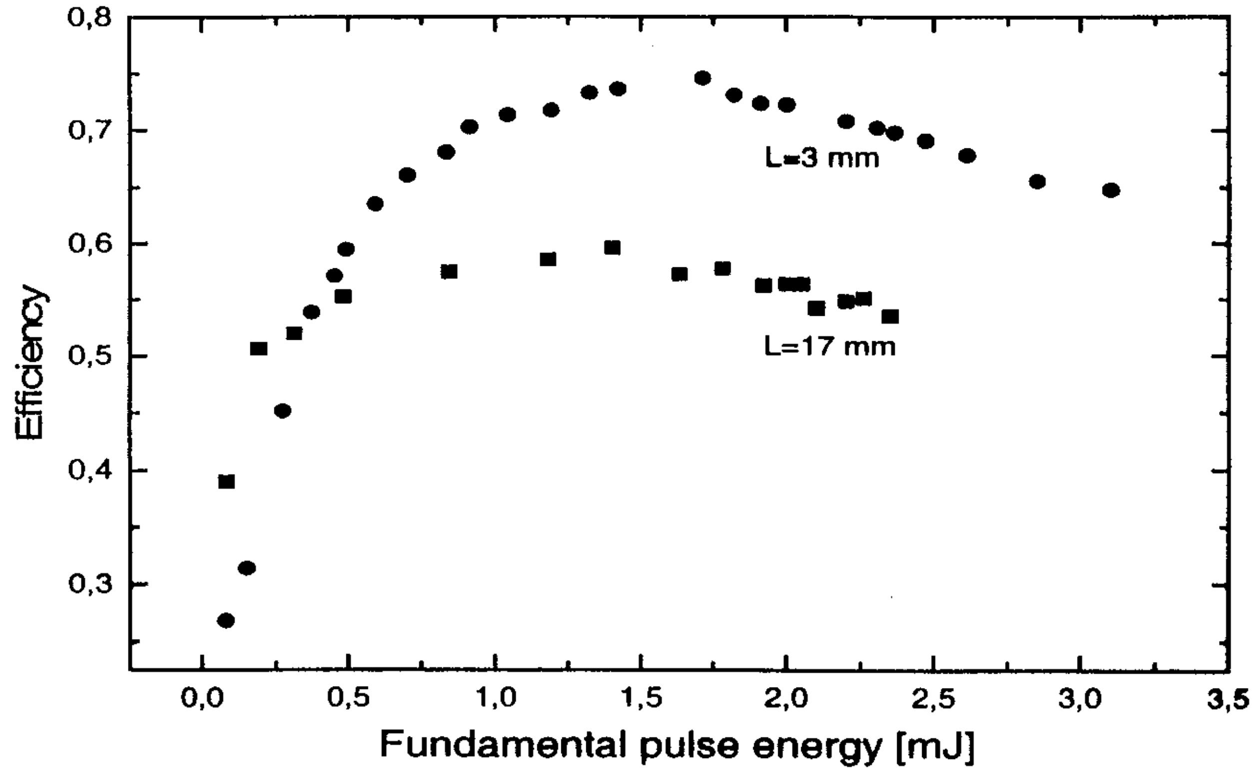

Measurements of Bulk Optical Damage in PPKTP

Fundamental Wavelength (λ_ω)	Crystal Length (L)	Pulse Length (τ_ω)	Repetition Rate (f)	Fundamental peak Intensity (I_ω)	Damage Behavior
1064 nm	10 mm	220 ns	1.2 kHz	71 MW/cm^2	Permanent
1064 nm	3 mm	5 ns	20 Hz	700 MW/cm^2	None
1064 nm	3 mm	5 ns	Single pulse	800 MW/cm^2	None
1064 nm	10 mm	100 ps	100 MHz	31 MW/cm^2	Scattering
780 nm	10 mm	100 fs	80 MHz	3 GW/cm^2	None

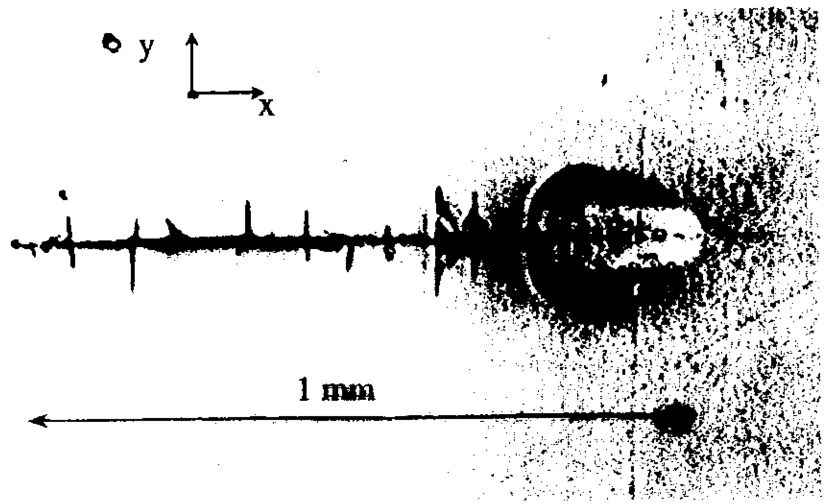

Broadly tunable mid-IR radiation source based on difference frequency mixing of high power wavelength-tunable laser diodes in bulk periodically poled $LiNbO_3$

S. Sanders, R.J. Lang, L.E. Myers, M.M. Fejer and R.L. Byer

Indexing terms: Semiconductor junction lasers, Lithium niobate

Coherent mid-IR radiation throughout the 3.6 to 4.3μm wavelength range is generated by difference frequency mixing (DFM) of wavelength-tunable laser diodes in periodically-poled $LiNbO_3$ (PPLN). Mid-IR power levels up to 7.1μW and DFM conversion efficiencies up to 0.015%/Wcm are demonstrated.

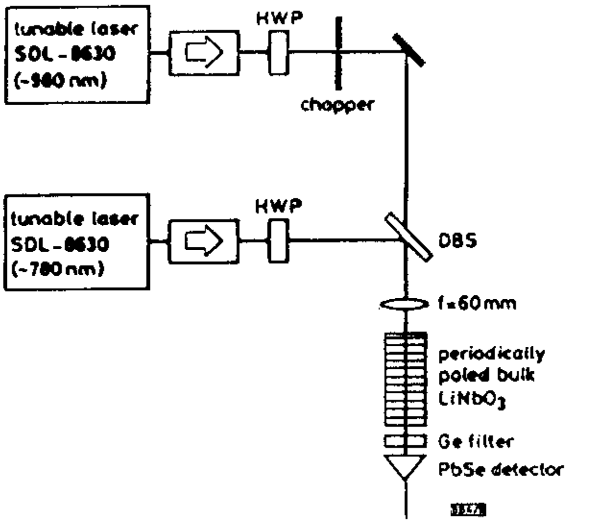

Fig. 1 *Schematic diagram of laser diode difference frequency mixing configuration*

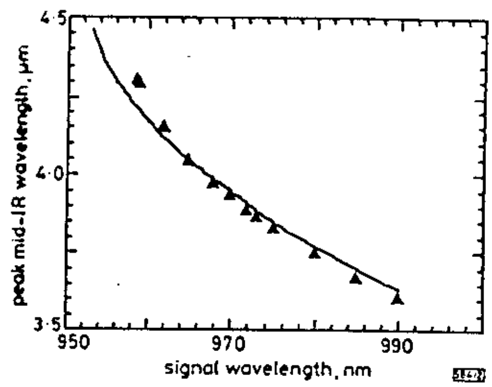

Fig. 2 *Peak mid-IR wavelength generated against signal wavelength for 21μm QPM period*

Pump wavelength is varied from 776 to 783nm to maintain phase-matching

▲ experimental points

——— theoretical phasematching wavelength

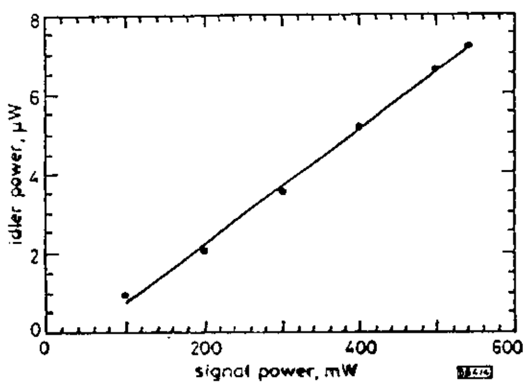

Fig. 4 *Generated idler power at 3.89μm wavelength against signal power*

λ_p = 777.7nm, λ_s = 972nm, λ_i = 389μm, P_p = 510mW

532 nm pumped optical parametric oscillator in bulk periodically poled lithium niobate

V. Pruneri,[a] J. Webjörn,[b] P. St. J. Russell, and D. C. Hanna
Optoelectronics Research Centre, University of Southampton, Southampton SO17 1BJ, United Kingdom

(Received 12 April 1995; accepted for publication 7 August 1995)

We report a quasi-phase-matched optical parametric oscillator (OPO) pumped by the second harmonic of a single frequency Q-switched Nd:YAG laser. Both the frequency doubling to 532 nm and the parametric oscillation are performed in periodically poled lithium niobate crystals with a nonlinearity of ~15 pm/V. The OPO has been operated in "singly resonant" and "doubly resonant" configurations. The threshold in the singly resonant case was ~0.14 J/cm², more than one order of magnitude below the damage limit. OPO tuning from 945 to 1225 nm was achieved by changing both the period of domain reversal (from 6.8 to 6.85 μm) and the temperature of the crystal. © *1995 American Institute of Physics.*

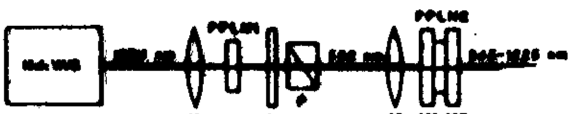

FIG. 2. Experimental setup of OPO: L: half-wave plate at 0.532 μm, P: polarizer, f1=75 mm, f2=32 mm, M1 and M2: plane mirrors.

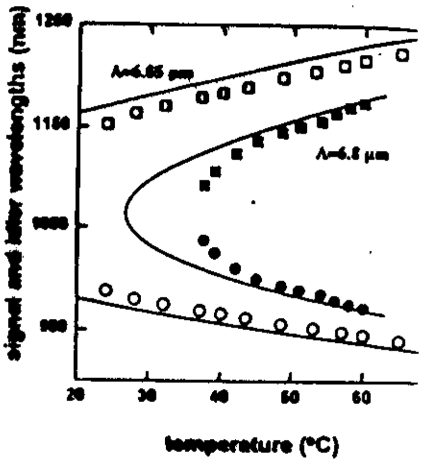

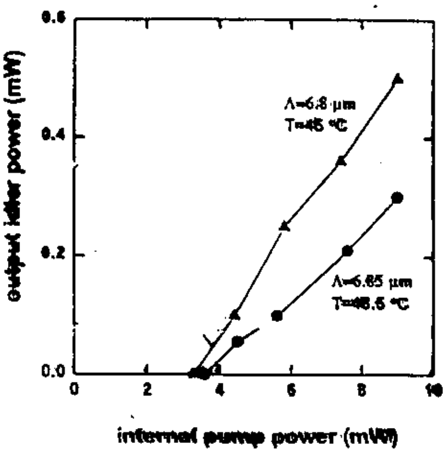

FIG. 5. Output of the SRC as a function of the internal pump power for two different periods of domain reversal, at two different temperatures.

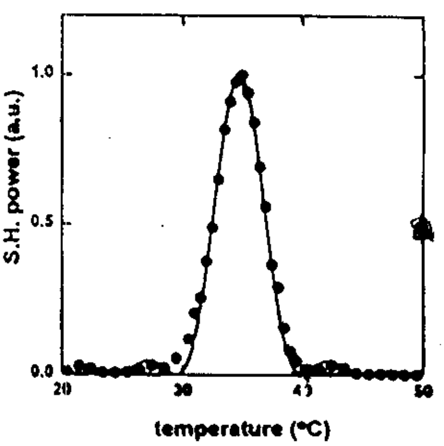

FIG. 1. SH power as function of the crystal temperature for sample PPLN1. The solid curve is a calculated curve for a perfect crystal of the same length.

SPF :

Pulse energy output @ 1.57 µm from 20 ns OPO based on 3 mm thick periodically poled RTA

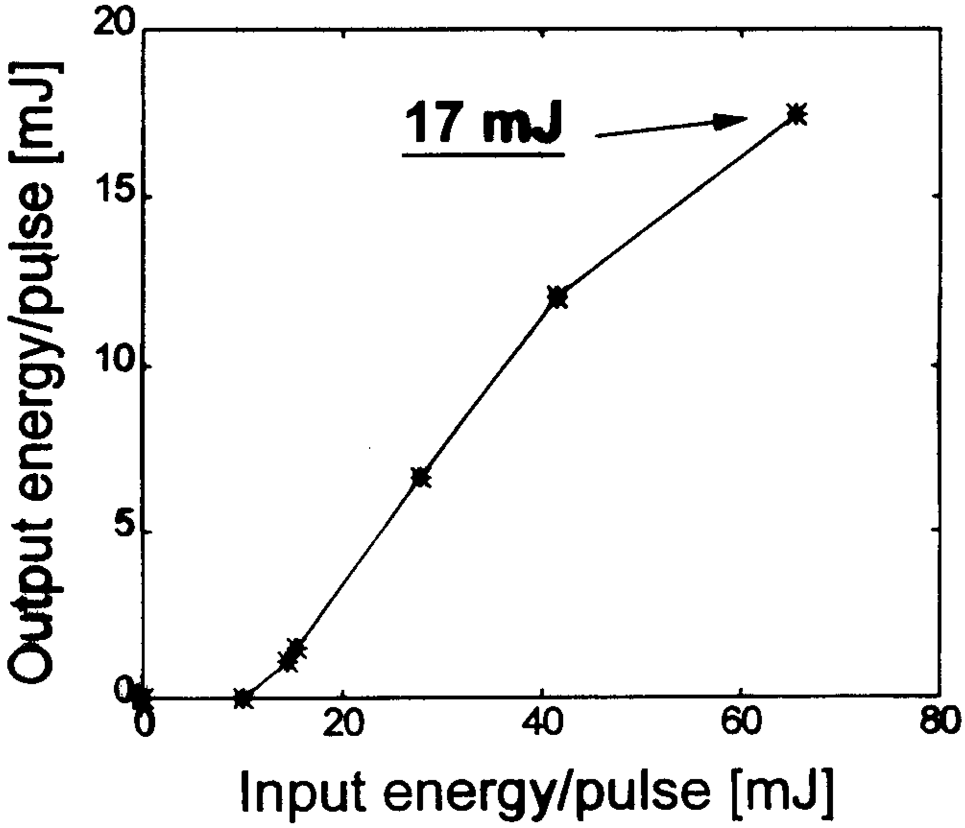

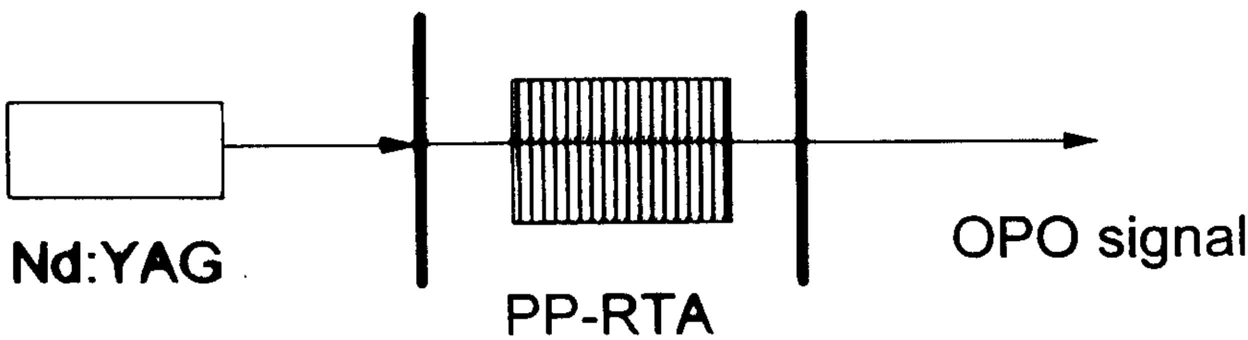

H Karlsson (AB IOF), S Wickström (SAAB Dynamics AB)

Conclusions

Periodically poled $KTiOPO_4$

- Suitable for nanosecond optical parametric oscillators
- High gain => efficient OPO
- Stable performance
- Large aperture => Extract higher energy pulses
- Operation at room-temperature
- No crystal damage occurred (900 MW/cm^2)

KTH

Continuous tuning of a continuous-wave periodically poled lithium niobate optical parametric oscillator by use of a fan-out grating design

P. E. Powers, Thomas J. Kulp, and S. E. Bisson

Combustion Research Facility, Sandia National Laboratories, Livermore, California 94550

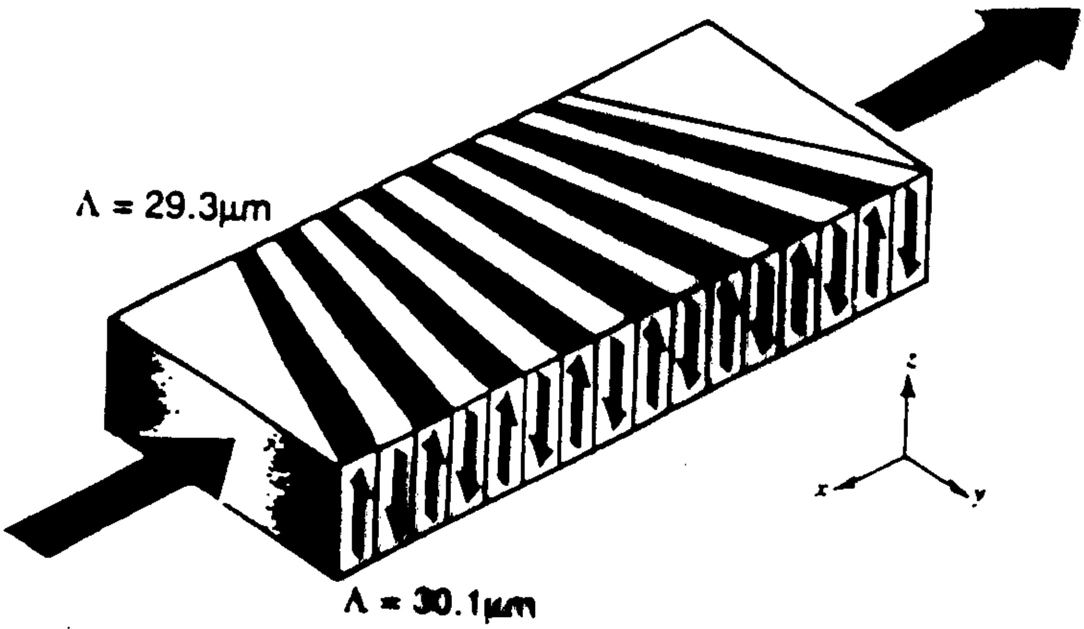

Fig. 1. Exaggerated view of the fan-out pattern on the PPLN crystal. The arrows on the side of the crystal indicate the poling direction. For the OPO the pump, signal, and idler beams are polarized along the crystallographic z axis (as indicated by the coordinates at the lower right), and they propagate along the x axis (as indicated by the large arrows entering and leaving the crystal), sampling only one periodicity.

2.5-W, continuous-wave, 629-nm solid-state laser source

Walter R. Bosenberg, Jason I. Alexander, Lawrence E. Myers, and Richard W. Wallace

Lightwave Electronics Corporation, Mountain View, California

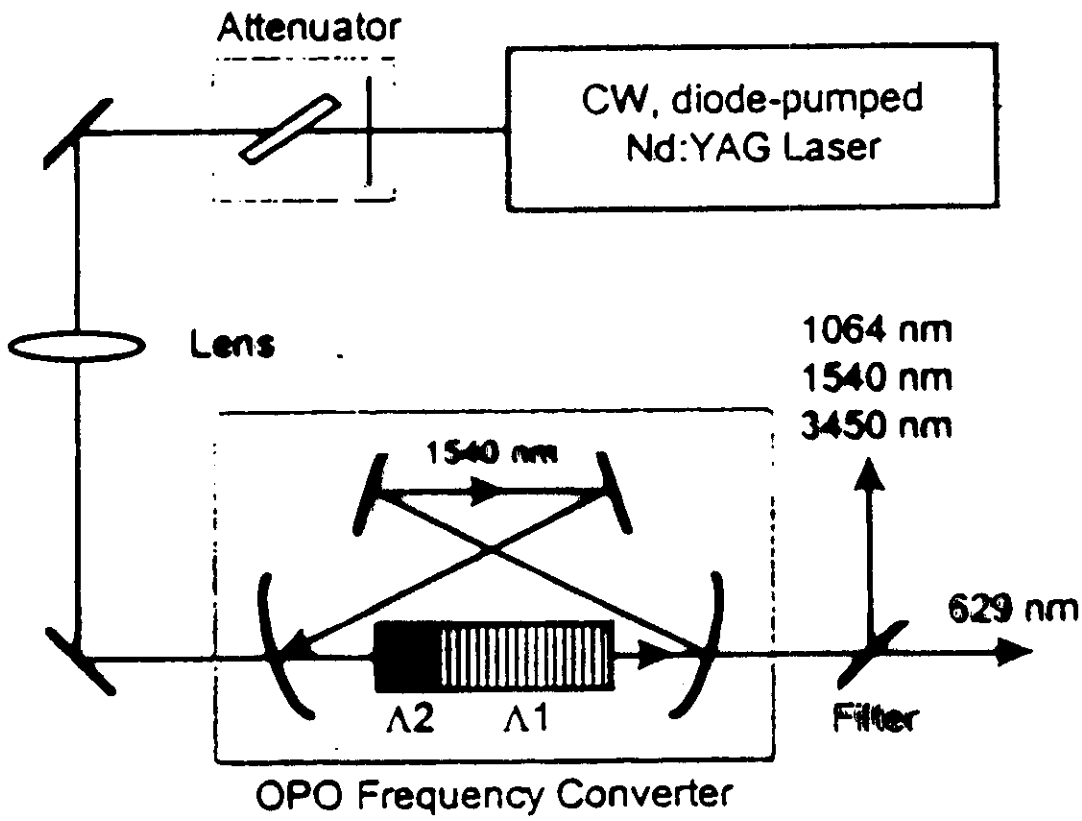

Fig. 1. Schematic of the experimental configuration. A cw Nd:YAG laser is used to pump the OPO frequency converter. The converter contains a dual-grating PPLN crystal ($\Lambda 1 = 29.2\ \mu m$ for phase matching 1064 nm → 1540 nm + 3450 nm; $\Lambda 2 = 11.0\ \mu m$ for phase matching 1064 nm + 1540 nm → 629 nm). A four-mirror ring cavity resonates the 1540-nm light. A dielectric coating filter is used to separate the various output wavelengths.

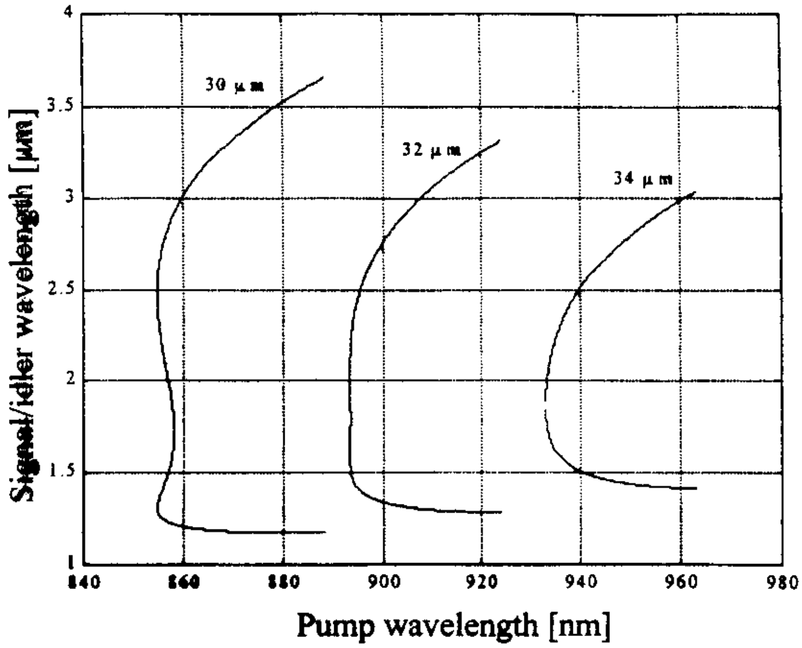

30 μm
32 μm
34 μm
Signal/idler wavelength [μm]
Pump wavelength [nm]

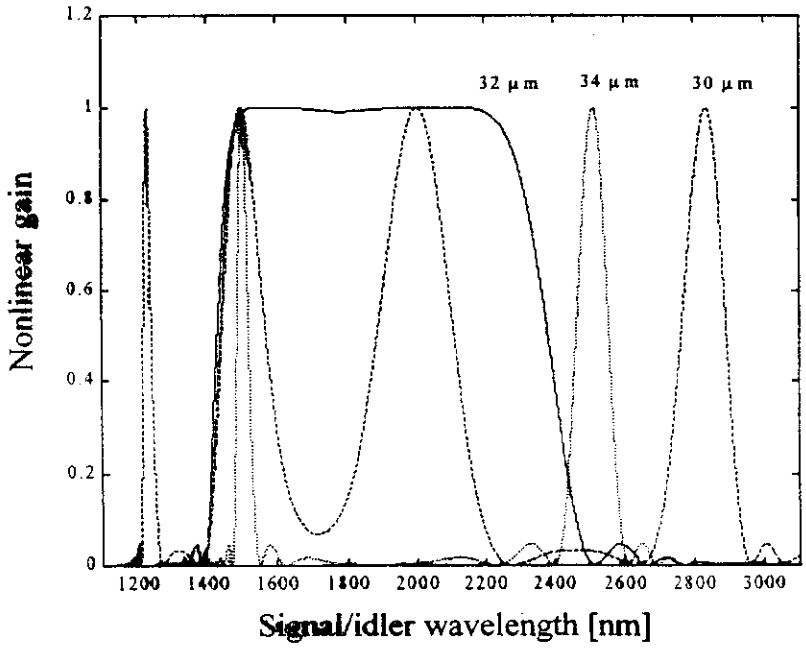

32 μm
34 μm
30 μm
Nonlinear gain
Signal/idler wavelength [nm]

Nonlinear Coefficient

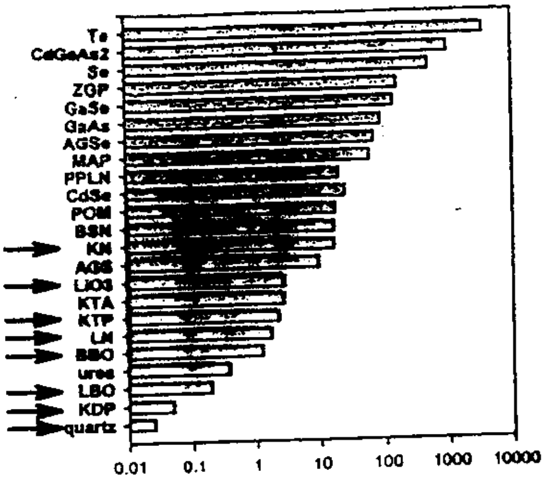

→ = used in commercial device

- Value of d_{eff} depends on angles of propagation & polarization and on wavelengths

Units of d_{eff} ~ pm/V

Figure of Merit = $\frac{d_{eff}^2}{n^3}$

- Commercially used materials have lower nonlinear coefficients
- High nonlinear coefficient does not necessarily make material useful

Requirements of NLO Materials for Frequency Conversion

- **Phasematching** -- limits useful interactions & applicability
- **Transmission** -- interacting waves not absorbed or scattered
- **Nonlinearity** -- non-centrosymmetric materials for $\chi^{(2)}$
- **Homogeneity** -- uniformity 1 part in 10^{-5}
- **Damage** -- absolute & relative to operating point
- **Mechanical properties** -- growing, polishing, coating
- **Thermal properties** -- dn/dT, thermal conductivity
- **Lifetime** -- chemical stability, hygroscopic, aging in use
- **Lack of "weirdness"** -- photorefractive, gray tracking
- **Availability** -- size, cost, uniformity of properties

All requirements must be simultaneously satisfied!

L. Myers

Multiple-channel wavelength conversion by use of engineered quasi-phase-matching structures in $LiNbO_3$ waveguides

M. H. Chou, K. R. Parameswaran, and M. M. Fejer

E. L. Ginzton Laboratory, Stanford University, Stanford, California 94305-4085

I. Brener

Bell Laboratories, Lucent Technologies, 700 Mountain Avenue, Murray Hill, New Jersey 07974

Received April 22, 1999

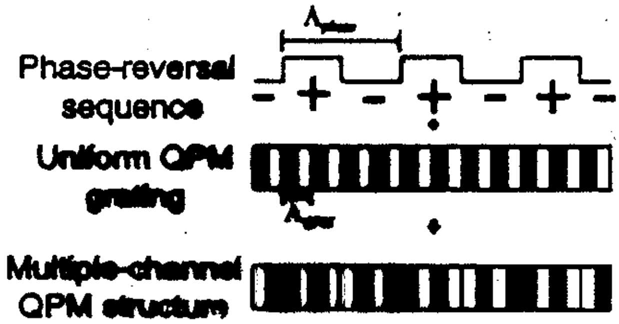

Fig. 1. Multiple-channel QPM structure formed by superimposition of a phase-reversal grating upon a uniform QPM grating.

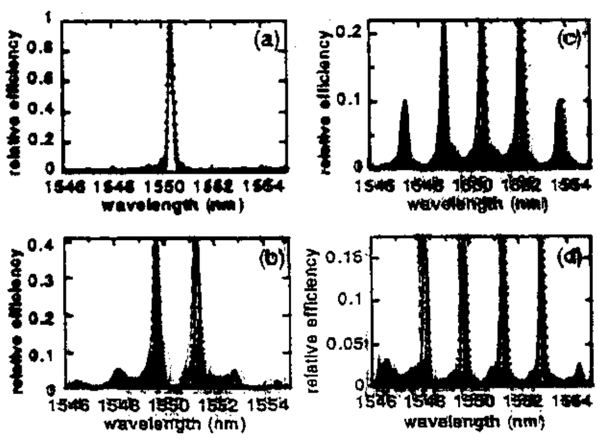

Fig. 2. SHG wavelength-tuning curves for (a) one-channel, (b) two-channel, (c) three-channel, and (d) four-channel devices. The filled circles are measured results, and the solid curves are theoretical fits. The efficiencies are relative to the peak efficiency (~600%/W) of a one-channel device.

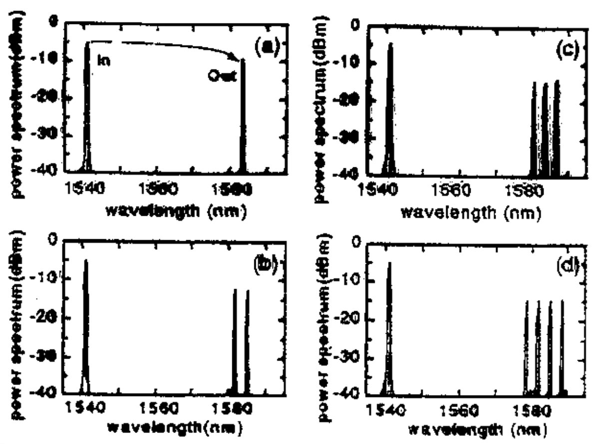

Fig. 3. Measured multiple-channel wavelength conversion of (a) one-channel, (b) two-channel, (c) three-channel, and (d) four-channel devices. Wavelength conversions of the individual channels were combined to form these plots.